

**РАДІОЕЛЕКТРОНІКА
ТА ТЕЛЕКОМУНІКАЦІЇ**
**RADIO ELECTRONICS
AND TELECOMMUNICATIONS**
**РАДИОЭЛЕКТРОНИКА
И ТЕЛЕКОММУНИКАЦИИ**

UDC 621.396

**RADAR CROSS-SECTION IMAGING IN SYNTHETIC APERTURE RADAR
WITH LINEAR ANTENNA ARRAY AND ADAPTIVE RECEIVER**

Volosyuk V. K. – Dr. Sc., Professor, Professor of the Aerospace Radio-Electronic Systems Department, National Aerospace University “Kharkiv Aviation Institute”, Kharkiv, Ukraine.

Zhyla S. S. – PhD, Head of the Aerospace Radio-Electronic Systems Department, National Aerospace University “Kharkiv Aviation Institute”, Kharkiv, Ukraine.

Ruzhentsev M. V. – Dr. Sc., Professor, Leading researcher of the Aerospace Radio-Electronic Systems Department, National Aerospace University “Kharkiv Aviation Institute”, Kharkiv, Ukraine.

Sobkolov A. D. – Postgraduate student of the Aerospace Radio-Electronic Systems Department, National Aerospace University “Kharkiv Aviation Institute”, Kharkiv, Ukraine.

Tserne E. O. – Assistant of the Aerospace Radio-Electronic Systems Department, National Aerospace University “Kharkiv Aviation Institute”, Kharkiv, Ukraine.

Kolesnikov D. V. – Engineer of the Aerospace Radio-Electronic Systems Department, National Aerospace University “Kharkiv Aviation Institute”, Kharkiv, Ukraine.

Vlasenko D. S. – Assistant of the Aerospace Radio-Electronic Systems Department, National Aerospace University “Kharkiv Aviation Institute”, Kharkiv, Ukraine.

Topal M. S. – Associate Professor of the Department of Airplanes and Helicopters Design, National Aerospace University “Kharkiv Aviation Institute”, Kharkiv, Ukraine.

ABSTRACT

Context. There are a large number of RCS estimation methods in synthetic-aperture radars (SAR), which differ by precision, RCS recovery time of an observation area and complexity of implementation. At the same time, the optimal method, which is a generalization of all existing ones and characterizes both spatial and temporal optimal signal processing, has not been synthesized. Also, usually problem statements do not take into account the stochastic structure of signals reflected from most underlying surfaces. As a result, further ways of improving resolution, optimal SAR structure and maximum achievable precision of estimation of RCS are not determined.

Objective. The goal of the work is to solve the problem of synthesis of the optimal method of RCS surfaces restoration as a statistical characteristic of spatially-inhomogeneous random scattering coefficient in aerospace-based radio engineering systems with moving linear antenna arrays and adaptive spatio-temporal signal processing.

Method. Applying the method of maximum likelihood estimation and taking into account a priori information about the statistical characteristics of the received spatio-temporal fields a super-resolution method of RCS estimation on spatial coordinates is derived. The generalized problem statement has shown the optimal method of surface observation that allows to overcome the contradiction between the size of the observation area and the accuracy of the parameter estimates. The obtained method allows to achieve highest resolution (as for SpotLight mode) of radar images for wide area of observation (as for Stripmap mode). It is shown that the general algorithm can be adapted to particular solutions with limited statements of the problem. In contrast to the well-known method of aperture synthesis the processing of the received field in the antenna array and receiver is adaptive and depends on the signal-to-noise ratio.

Results. The optimal method of area scanning in onboard SAR with antenna arrays and the corresponding method of adaptive spatio-temporal signal processing can be used to describe the receiving path of cognitive on-board radar for remote sensing.

Conclusions. The obtained optimal method can be considered as a modified method of aperture synthesis with a multi-beam spotlight mode with the possibility of adaptive radiation pattern formation and signal time processing. In contrast to the classical method performing matched-filtering of the received signal with the reference signal, the modified method additionally decorrelates signals reflected from the earth’s surface. As a result of this decorrelation the characteristic intervals of speckles (the size of the spotted pattern of the image) will be significantly smaller than with match-filtering. Therefore, their subsequent smoothing with the same efficiency can be performed by windows of smaller width. Such processing together with a multi-beam spotlight mode will significantly increase the resolution of the SAR with an expanded area of view.

KEYWORDS: synthetic aperture radar, radar cross section, statistical optimization, optimal acquisition mode, superresolution method, cognitive radars.

ABBREVIATIONS

RCS is a radar cross section;

SAR is a synthetic-aperture radar;

ScanSAR is a scanning synthetic aperture radar;

TOPS is a terrain observation with progressive scan;

ITOPS is an inverse terrain observation with progressive scan.

NOMENCLATURE

\otimes is a convolution operator;

$(\cdot)^*$ is a complex conjugation operator;

$A(\cdot)$ is an envelope of the probing signal;

$\dot{A}(\cdot)$ is a complex envelope of the probing signal;

c is a speed of light in vacuum;

D is an observation area;

D' is an antenna surface;

$d\vec{r}$ is a surface element of the D ;

$d\vec{r}'$ is a surface element of the D' ;

$E_W(\vec{r})$ is an energy of the reference signal;

$\dot{F}(\vec{r})$ is a complex scattering coefficient of $d\vec{r}$;

$F_{x'}\{\cdot\}$ is a discrete Fourier transform in spatial coordinates;

$F_{x'}^{-1}\{\cdot\}$ is an inverse discrete Fourier transform in spatial coordinates;

$F_T^{-1}\{\cdot\}$ is a Fourier transform in time coordinates;

$F_T^{-1}\{\cdot\}$ is an inverse Fourier transform in time coordinates;

$\dot{F}_{D'}(\cdot)$ is a radiation pattern of the antenna;

f_0 is a central frequency;

$G_R(\cdot)$ is a two-dimensional Fourier transform of correlation function $R_u(\cdot)$;

$G_W(\cdot)$ is a two-dimensional Fourier transform of inverse correlation function $W(\cdot)$;

$G_{WD}(\cdot)$ is a spectral characteristic of adaptive inverse filter for spatial processing;

$G_{WT}(\cdot)$ is a spectral characteristic of adaptive inverse filter for time processing;

H is an aircraft flight altitude;

$\dot{I}(x')$ is a complex amplitude-phase distribution;

\dot{I}_n is an amplitude-phase distribution for antenna array;

$\dot{I}_{Wmk}(\cdot)$ is an optimal amplitude-phase distribution of the transfer coefficient of the elements of the antenna array;

$\text{Im } \dot{F}(\vec{r})$ is an imaginary part of the complex scattering coefficient;

j is a unit imaginary number;

k is a wave number;

N_{0n} is a power spectral density;

$n(\cdot)$ is a white internal noise;

$P(x, y)$ is a point on the surface with coordinates x, y ;

$P[u(t, x') | \sigma^0(\vec{r})]$ is a likelihood functional;

$R_0(\vec{r}, t)$ is a range to surface element \vec{r} for time t ;

$\dot{R}_F(\cdot)$ is a correlation function of the scattering coefficient $\dot{F}(\vec{r})$;

$R_n(\cdot)$ is a correlation function of a white noise;

$R_u(\cdot)$ is a final correlation function for cognitive SAR;

$\vec{r} = (x, y)$ is a coordinate of the surface element;

$\text{Re } \dot{F}(\vec{r})$ is a real part of the complex scattering coefficient;

$\dot{s}_0(t)$ is a unit signal;

$\dot{S}_0(j\omega)$ is a spectrum of $\dot{s}_0(t)$;

$s_t(t)$ is a signal transmitted in the direction of the surface;

$\dot{s}(t, x')$ is a signal, received by the registration area;

$\dot{s}_{0W}(\cdot)$ is a pulse response of the optimal and adaptive spatio-temporal filter;

T is an observation time;

t is a time;

$t_d(\vec{r}, x')$ is a signal delay time during propagation from the transmitting antenna to the surface and vice versa;

$\dot{U}(j\omega)$ is a spectrum of the observation equation;

$\dot{u}(\cdot)$ is a complex envelope of the observation equation;

$u(\cdot)$ is an observation equation;

$u_m(t_1)$ is an observation equation for antenna array;

V is a velocity of the aircraft;

$W(\cdot)$ is an inverse correlation function;

$W_{mn}(\cdot)$ is an adaptive inverse correlation matrix of the received signals in space;

$W_T(\cdot)$ is an inverse correlation function in time;

x' is a coordinate of each element of the antenna;

x'_n is a coordinate of n -th element of the antenna array;

$\dot{Y}(\vec{r})$ is an optimal output effect for continuous antenna;

$\dot{Y}_k(\vec{r})$ is an optimal output effect for antenna array;

$\delta(\cdot)$ is a delta function;

ϵ is an attenuation of the signal along the propagation path;

$\theta_x(\cdot)$ is an azimuth angle;

$\theta_{xk}(\cdot)$ is a discrete value of k -th azimuth angle;

$\vartheta_x(\cdot)$ is the direction cosine of the coordinate x ;

$\vartheta_{xk}(\cdot)$ is a discrete value of k -th direction cosine;

ϑ_x is a vector of direction cosines;

$\kappa[\sigma^0(\vec{r})]$ is a coefficient in the likelihood functional depending on the desired energy parameter $\sigma^0(\vec{r})$;

$\hat{\lambda}(\vec{r})$ is an estimated parameter;

$\sigma^0(\cdot)$ is a RCS for scattering surface;

ϕ is an initial phase;

$\Psi_W(\cdot)$ is a complex ambiguity function;

ω_0 is a circular frequency.

INTRODUCTION

Synthetic-aperture radars are a key component of the modern aerospace equipment for aircraft and artificial Earth satellites. The images formed by them are in high demand due to high resolution, commensurate with optical images, weatherproof and non-dependent time of day measurements. At present, space SARs implement a significant number of views (high-precision Spotlight Mode, wide-range strip Strip-map Mode, multi-view mode, etc.), use planar phased antenna arrays for measurements, process signals by advanced methods of digital signal processing. From the analysis of their technical characteristics it follows that the spatial resolution of radar images is constantly improving and has already reached a sub-meter value. At the same time, the variety of technical solutions and methods of forming an artificial aperture of an antenna in moving radars does not have an optimal theory of creating methods and means of spatio-temporal signal processing. This, in turn, imposes restrictions on the creation of cognitive radars with optimal spatio-temporal signal processing. Also, the synthesis of new methods usually does not take into account the stochastic nature of reflected signals from real underlying surfaces, which limits the potential characteristics of SAR. Consequently, the problem of optimization of spatio-temporal signal processing in modern on-board SARs, synthesis of new methods of estimation of RCS of surface as a statistical characteristic of the complex scattering coefficient and determination of the potential of radar systems with antenna array located on aerospace carriers are relevant.

The object of study is the process of radar imaging of surfaces as a statistical characteristic of their random scattering coefficient.

The subject of study is the methods and devices for optimal spatio-temporal signal processing in SAR with linear antenna arrays.

The known methods [1–25] are synthesized with already specified spatial processing of signals in an antenna array, that is given in problem statement, without the possibility of its change, which does not allow to obtain a generalized method with the best resolution and extended area of observation. Also, existing methods do not take into account the statistical characteristics of the reflected signals from surfaces and the possibilities of adaptive processing in spatial and time.

The purpose of the work is to increase spatial resolution and expand the area of observation of the SAR, using modern achievements of the statistical theory of optimization of radio engineering systems.

1 PROBLEM STATEMENT

Suppose that on the board of an aircraft moving straight at a constant velocity V and height H , there is a linear array antenna with coordinates (x', z) , as it is shown in Fig. 1. The coordinates of the phase center of the antenna at an arbitrary point in time t are equal to $(x = Vt, y = 0, z = H)$. A signal is transmitted in the direction of the observation area D , in a wide sector of angles

$$s_t(t) = A(t)\cos(2\pi f_0 t + \phi) = \operatorname{Re}\{\dot{A}(t)e^{j\omega_0 t}\}. \quad (1)$$

In the general case $\dot{A}(t)$ represents a wide class of radio engineering signals, both simple and complex (with modulation).

Transmitted signal reaches the surface D with coordinates $\vec{r} = (x, y, 0) \in D$, reflects from it (scattered by its inhomogeneities) and is received by each element of the antenna with coordinates x' and a complex amplitude-phase distribution $\dot{I}(x')$.

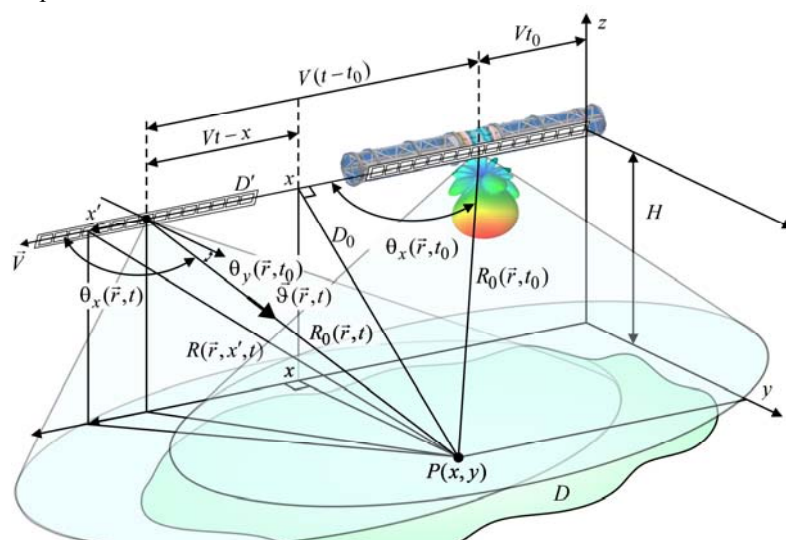


Figure 1 – Geometry of the underlying surface observation

The signals received by the registration area are stochastic and have the following form [26, 27]:

$$\dot{s}(t, x') = \int_D \dot{F}(\vec{r}) \dot{s}_0(t, \vec{r}, x') d\vec{r}, \quad (2)$$

where

$$\dot{s}_0(t, \vec{r}, x') = \varepsilon \dot{I}(x') \dot{A}(t - t_d(\vec{r}, x')) \times \\ \times \exp[j2\pi f_0(t - t_d(\vec{r}, x'))], \quad (3)$$

– unit signal reflected from a surface element $d\vec{r}$ with $\dot{F}[\vec{r}, \lambda(\vec{r})] = 1$. From the analysis of Fig. 1 it follows that the signal (3) with the rectilinear motion of the aircraft with constant velocity V has the form

$$\dot{s}_0(t, \vec{r}, x') = \varepsilon \dot{I}(x') \exp(j2k\vartheta_x(\vec{r}, t)x') \dot{A}(t - 2R_0(\vec{r}, t)c^{-1}) \times \\ \times \exp(-jkV^2(t - t_0)^2 R_0^{-1}(\vec{r}, t_0) \sin^2 \theta_x(\vec{r}, t_0)) \times \\ \times \exp(j2k(Vt - Vt_0) \cos \theta_x(\vec{r}, t_0)) \exp(j2\pi f_0 t). \quad (4)$$

There is internal noise in any receiver that is why we write the observation equation in the following form

$$u(t, x') = \operatorname{Re} \dot{s}(t, x') + n(t, x'), \quad (5)$$

where $n(t, x')$ is a white internal noise with a correlation function

$$R_n(t_1, t_2, x'_1, x'_2) = 0,5N_{0n} \delta(t_1 - t_2) \delta(x'_1 - x'_2). \quad (6)$$

The correlation function of the scattering coefficient $\dot{F}(\vec{r})$ for the most practical problems of terrain mapping has the form

$$\dot{R}_F(\vec{\eta}_1, \vec{\eta}_2) = \langle \dot{F}(\vec{\eta}_1) \dot{F}^*(\vec{\eta}_2) \rangle = \sigma^0(\vec{\eta}_1) \delta(\vec{\eta}_1 - \vec{\eta}_2). \quad (7)$$

For our problem $\sigma^0(\vec{r})$ is an estimated parameter, the desired image.

Taking into account (2), (6) and (7), we present the correlation function of (5) in the following form

$$R_u(t_1, t_2, x'_1, x'_2, \sigma^0(\vec{r})) = \langle u(t_1, x'_1) u(t_2, x'_2) \rangle = \\ = 0,5 \operatorname{Re} \int_D \sigma^0(\vec{r}) \dot{s}_0(t_1, \vec{r}, x'_1) \dot{s}_0^*(t_2, \vec{r}, x'_2) d\vec{r} + \\ + 0,5N_{0n} \delta(t_1 - t_2) \delta(x'_1 - x'_2). \quad (8)$$

This correlation function contains all the necessary information for the adaptive work of cognitive SAR.

According to the reception of stochastic reflected signals $\dot{s}(t, x')$ by each element of the antenna array D' ,

observed against the background of additive Gaussian noises $n(t, x')$, it is necessary to optimally estimate the RCS $\sigma^0(\vec{r})$ of the underlying surface as a statistical characteristic of the complex scattering coefficient $\dot{F}(\vec{r})$ using onboard radar with linear antenna array.

2 REVIEW OF THE LITERATURE

The method of artificial synthesis of an aperture of an antenna located on board of the aircraft was proposed approximately 70 years ago [1]. Since then, methods of area scanning [2–6], technical means of implementing spatio-temporal signal processing [7–9], a set of orthogonal probing signals [12, 13], post-processing of SAR images [14, 15] and applications of these images [16–18] have been constantly developing. At the same time, most of the results presented are obtained more as a generalization of engineering experience in operation and development of such systems, rather than as a result of solving statistical problems of optimization of radio devices and systems. As a result, the further development of high-precision SAR for a long time could not exceed the decimeter resolution [19–21]. In recent years, developers of the RAMSES-NG system have succeeded in building a radar image with a subdecimeter resolution [22, 23]. Such results have been achieved through the use of the full potential of the frequency range, which covers the waveguide. The improvement in accuracy leads to decreasing the observation area and increasing the global monitoring time. Such a contradiction has long been known in the practice of aerospace radio-vision. Possible ways of further development are noted in the works [24, 25]. The presented radar schemes are logical and will give results in practice, but at the same time, this approach does not allow to determine the potential (best) method of spatio-temporal signals and will reveal further ways of development. It should also be noted that most algorithms do not take into account the stochastic nature of signal reflection from most underlying surfaces, which is also informative for further optimization of SAR systems.

In contrast to the above results, it is proposed to synthesize an optimal method of RCS estimation for underlying surfaces as a statistical characteristic of their random complex scattering coefficient in onboard radars with linear antenna arrays. It is proposed to use modern methods [28] of statistical optimization and decision theory to optimize the radar structure.

3 MATERIALS AND METHODS

We can obtain the optimal method of the $\sigma^0(\vec{r})$ estimation by the maximum likelihood method. We will write the likelihood functional for the stochastic model of received signals, as shown in [29–32], in the following form:

$$P[u(t, x') | \sigma^0(\vec{r})] = \kappa[\sigma^0(\vec{r})] \exp\left\{-\frac{1}{2} \int \int \int \int u(t_1, x'_1) \times \right. \\ \left. \times W(t_1, t_2, x'_1, x'_2, \sigma^0(\vec{r})) u(t_2, x'_2) dt_1 dt_2 dx'_1 dx'_2\right\}, \quad (9)$$

where $W(t_1, t_2, x'_1, x'_2, \sigma^0(\vec{r}))$ is found from the inverse integral equation

$$\int \int R_u(t_1, t_2, x'_1, x'_2, \sigma^0(\vec{r})) \times \\ \times W(t_2, t_3, x'_2, x'_3, \sigma^0(\vec{r})) dx'_2 dt_2 = \delta(t_1 - t_3) \delta(x'_1 - x'_3). \quad (10)$$

Applying the variational derivative to (10)

$$\frac{\delta \ln P[u(t, x') | \sigma^0(\vec{r})]}{\delta \sigma^0(\vec{r})} \Bigg|_{\sigma^0(\vec{r})=\sigma_{opt}^0(\vec{r})} = 0 \quad (11)$$

we obtain the likelihood equation

$$|\dot{Y}(\vec{r})|^2 = \frac{1}{2} \int_D \sigma^0(\vec{r}_1) |\dot{\Psi}(\vec{r}, \vec{r}_1)|^2 d\vec{r}_1 + N_{0n} E_W(\vec{r}). \quad (12)$$

The left side (12) is the optimal method for processing received signals

$$\dot{Y}(\vec{r}) = \int \int u(t_1, x'_1) \dot{s}_{0W}[t_1, x'_1, \sigma^0(\vec{r})] dx'_1 dt_1, \quad (13)$$

the essence of which is the matched filtering of the received oscillations in the optimal and adaptive spatio-temporal filter with a pulse response

$$\dot{s}_{0W}[t_1, x'_1, \sigma^0(\vec{r})] = \\ = \int \int W(t_1, t_3, x'_1, x'_3, \sigma^0(\vec{r})) \dot{s}_0(t_3, \vec{r}, x'_3) dx'_3 dt_3. \quad (14)$$

Expression (13) form the basis of the modified aperture synthesis method in airborne radars with antenna arrays. In contrast to the classical method, the modified one additionally performs decorrelation of signals reflected from the earth's surface in the adaptive filter $W(t_1, t_3, x'_1, x'_3, \sigma^0(\vec{r}))$. As a result of this, the speckle intervals (spot sizes) of radar images will be significantly smaller than with classical aperture synthesis. Therefore, their subsequent smoothing with the same efficiency can be performed with windows of smaller width, which ultimately allows to increase the resolution of the SAR.

The right side is the square-smoothed $\sigma^0(\vec{r}_1)$ by ambiguity function

$$\dot{\Psi}(\vec{r}, \vec{r}_1) = \int \int \dot{s}_0(t_1, \vec{r}, x'_1) \dot{s}_{0W}^*(t_1, \vec{r}_1, x'_1) dx'_1 dt_1 \quad (15)$$

and the offset estimate of the desired radar image by the amount $N_{0n} E_W(\vec{r})$, where

$$E_W(\vec{r}) = \frac{1}{2} \int \int |\dot{s}_{0W}(t_3, \vec{r}, x'_3)|^2 dx'_3 dt_3. \quad (16)$$

We will consider in more detail the structure of the unit signal and its effect on the processing of the received field $u(t, x')$, assuming that the antenna consists of a discrete set of isotropic emitters. In this case, the inverse correlation function can be factorized

$$W(t_1, t_3, x'_1, x'_3, \sigma^0(\vec{r})) = \\ = W_{mn}(t, \sigma^0(\vec{r})) \cdot W_T(t_1, t_3, \sigma^0(\vec{r})), m = \overline{1, M}, n = \overline{1, N}. \quad (17)$$

Substituting (4) and (17) into (13), we obtain the optimal output effect of a moving radar system with a linear antenna array in a vector-matrix form

$$\dot{Y}_l(\vec{r}) = \int \int \left[\sum_{n=1}^N \left(\sum_{m=1}^M u_m(t_1) W_{mn}(t_1, \sigma^0(\vec{r})) \right) \right] \dot{I}_n \times \\ \times \exp(j2k\vartheta_{xl}(\vec{r}, t_1) x'_n) \left] W_T(t_1, t_3, \sigma^0(\vec{r})) dt_1 e^{j2\pi f_0 t_3} \times \right. \\ \left. \times \exp(j2k(Vt_3 - Vt_0) \cos \theta_{xl}(\vec{r}, t_0)) \dot{A}(t_3 - 2R_0(\vec{r}, t_3)c^{-1}) \times \right. \\ \left. \times \exp\left(-jk \frac{V^2(t_3 - t_0)^2}{R_0(\vec{r}, t_0)} \sin^2 \theta_{xl}(\vec{r}, t_0)\right) dt_3. \quad (18) \right.$$

The essence of processing the space-time signals $u_m(t_1)$ received by the antenna array according to (18) is as follows. Firstly, the received oscillations from the output of each antenna array element are whitened in the spatial filter $W_{mn}(t_1, \sigma^0(\vec{r}))$. This is followed by the operation of compensating phase shifts of reflected signals from each point on the surface (multiplication by $\exp(j2k\vartheta_{xl}(\vec{r}, t_1) x'_n)$) and coherent summation with amplitude-phase distribution \dot{I}_n . These operations correspond to the operation of the adaptive beam-forming circuit, which forms a set of moving rays focused on each point on the surface. This type of review allows to increase the observation time and expand the range of viewing angles. The signals observed by each diagram in time are decorrelated in the filter with the impulse response $W_T(t_1, t_3, \sigma^0(\vec{r}))$, which leads to the broadening of the spectrum band of the observed oscillations. The broadening of band width is adaptive and depends on the amount of $\sigma^0(\vec{r})$. Multiplication by $\exp(j2\pi f_0 t_3)$ transfers the

observed signals to an intermediate frequency. Multiplication by the next exponent compensates the Doppler frequency shift of the reflected signals in the anterolateral and posterolateral observation. The next stage of processing is the coherent detection of amplitudes in the filter grating with impulse characteristics $\dot{A}(t_3 - 2R_0(\vec{r}, t_3)/c)$, each of which is tuned to the range $R_0(\vec{r}, t_3)$ in the case of impulse operation of the radar. The last exponent reveals the essence of the classical method of synthesis of the antenna aperture, which consists in the coherent accumulation of reflected signals with a quadratic phase shift along the flight path of the aircraft. Coherent phase shift in the reference signal leads to the formation of an artificial aperture, the length of which is equal to the product of the velocity of the aircraft and the synthesis time. In this case, the synthesis time is determined by the time of focusing on the selected point.

The described processing combines two methods antenna aperture synthesizing in the case of a Spot-Light and multi-look observation of the underlying surface. At the same time, it implements the advantages of each of them. The obtained method has the highest spatial resolution in azimuth (along the flight path) due to the constant focusing on the selected area of space and covers a significant area of the surface as a result of the formation of many partial antenna patterns.

The form of adaptive decorrelating filters in (18) and the whole method (18) depend on the signal-to-noise ratio, the type of the probing signal, the parameters of the antenna array, sounding geometry, and RCS of the studied one. This result gives a wide range of possible changes and can be used for describing of the receiving path of the cognitive radar.

The principle of the formation of a multiple rays, each of which focuses on a selected area of the underlying surface, followed by coherent processing of the path signal is shown in Fig. 2. The given geometries show the process of radar imaging of a surface with high spatial resolution without gaps.

For a physical interpretation of the decorrelation process in obtained algorithm (18), we divide the procedure of imaging into two stages: spatial and temporal processing.

Spatial processing. At coinciding moments in time $t_1 = t_3 = t$ (at the current time t), spatial processing is determined by the internal sums of expression (18)

$$\begin{aligned} \dot{Y}_{D'l}(t_1, \vec{r}) &= \sum_{n=1}^N \left(\sum_{m=1}^M u_m(t_1) W_{mn}(t_1, \sigma^0(\vec{r})) \right) \dot{I}_n \times \\ &\times \exp(j2k\vartheta_{xl}(\vec{r}, t_1)x'_n) = \sum_{m=1}^M u_m(t_1) \dot{I}_{Wml}(t_1, \vec{r}), \end{aligned} \quad (19)$$

where

$$\begin{aligned} \dot{I}_{Wml}(t_1, \vec{r}) &= \sum_{n=1}^N \dot{I}_n \exp(j2k\vartheta_{xl}(\vec{r}, t_1)x'_n) \times \\ &\times W_{mn}(t_1, \sigma^0(\vec{r})). \end{aligned} \quad (20)$$

The discrete Fourier transform in spatial coordinates $F_{x'}\{\cdot\}$ of (20) is the radiation pattern of the antenna system

$$\begin{aligned} F_{x'}\{\dot{I}_{Wml}(t_1, \vec{r})\} &= \\ = F_{x'}\{\dot{I}_n \exp(j2k\vartheta_{xl}(\vec{r}, t_1)x'_n)\} \cdot F_{x'}\{W_n(t_1, \sigma^0(\vec{r}))\}. \end{aligned} \quad (21)$$

The first factor is the radiation pattern $\dot{F}_{D'}(\vartheta_{xl}(\vec{r}, t_1))$ of an antenna with amplitude-phase distribution \dot{I}_n shifted on coordinate ϑ_x by the number of angles $\vartheta_{xl}(\vec{r}, t_1)$. Physically, this factor indicates the procedure for the formation of many radiation patterns oriented to each point on the surface \vec{r} and changing their angular direction as the aircraft moves creating a focusing effect at every point $P(x, y)$ of the surface. By selection \dot{I}_n the shape of the antenna pattern can be adjusted. This type of review allows to increase the observation time and expand the range of viewing angles. The second factor of expression (21) is an adaptive spatial decorrelation filter with a spatial characteristic

$$G_W(t_1, \vartheta_{xl}(\vec{r}, t_1)) = \frac{1}{\sigma^0(\vartheta_{xl}(\vec{r}, t_1)) |\dot{S}_0(t_1, \vartheta_{xl}(\vec{r}, t_1))|^2 + \frac{N_{0n}}{2}}. \quad (22)$$

where $\dot{S}_0(t, \vartheta_{xl}(\vec{r}, t))$ is the spectrum of (4).

Taking into account (22) the expression (19) will be

$$\begin{aligned} \dot{Y}_{D'l}(t, \vec{r}) &= \\ = F_{x'}^{-1} \left\{ \frac{\dot{u}(t, \vartheta_{xl}(\vec{r}, t)) \dot{F}_{D'}(\vartheta_{xl}(\vec{r}, t))}{\sigma^0(\vartheta_{xl}(\vec{r}, t)) |\dot{S}_0(t, \vartheta_{xl}(\vec{r}, t))|^2 + \frac{N_{0n}}{2}} \right\}. \end{aligned} \quad (23)$$

The numerator of expression (23) indicates the selectivity of the antenna array in angular coordinates in the form of a radiation pattern. The denominator extends the observation area limited by the antenna array radiation pattern due to inverse filtering in the adaptive filter $W_{mn}(t_1, \sigma^0(\vec{r}))$.

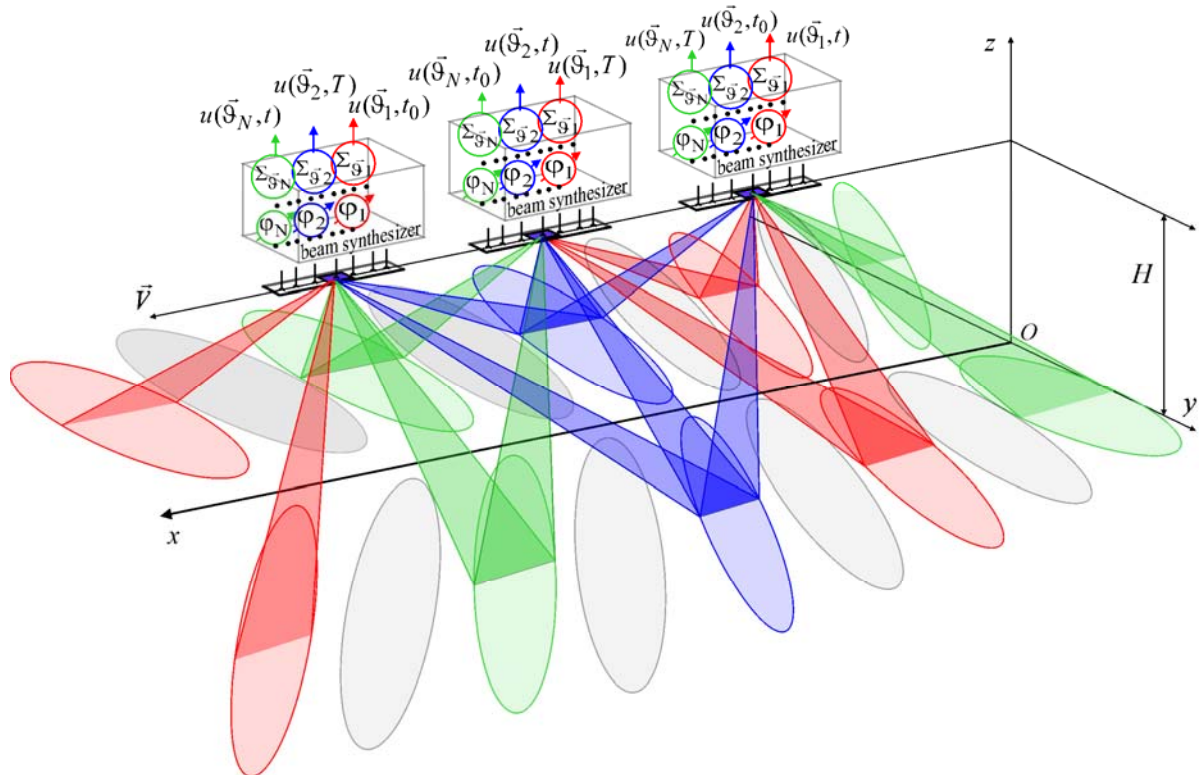


Figure 2 – The principle of the formation of a multiple radiation beams with coherent processing in each of them

Temporal processing. The temporal processing in (18) is defined at some point $x'_n = 0$, $n = m$ in the following form

$$\dot{Y}_l(\vec{r}) = \int_T^T u(t_1) \int_T^T \dot{s}_0(t_3, \vec{r}) W_T(t_1, t_3, \sigma^0(\vec{r})) dt_3 dt_1, \quad (24)$$

where

$$\begin{aligned} \dot{s}_0(t_3, \vec{r}) = & \dot{A}(t_3 - 2R_0(\vec{r}, t_3)c^{-1}) e^{j2\pi f_0 t_3} \times \\ & \times \exp(j2k(Vt_3 - Vt_0) \cos \theta_{xl}(\vec{r}, t_0)) \times \\ & \times \exp\left(-jk \frac{V^2(t_3 - t_0)^2}{R_0(\vec{r}, t_0)} \sin^2 \theta_{xl}(\vec{r}, t_0)\right). \end{aligned} \quad (25)$$

We will find the inverse correlation function using the inverse Fourier transform in temporal coordinates $F_T^{-1}\{\cdot\}$

$$\begin{aligned} W[\tau, \sigma^0(\vec{r})] &= F_T^{-1}\{G_R^{-1}[\omega, \sigma^0(\vec{r})]\} = \\ &= F_T^{-1}\{(\sigma^0(\vec{r}) |\dot{s}_0(j\omega)|^2 + 0.5N_{0n})^{-1}\}, \end{aligned} \quad (26)$$

where $G_R[\omega, \sigma^0(\vec{r})]$ is found at some point $x'_n = 0$, $n = m$.

Taking into account (26), algorithm (24) in spectral domain takes the form

$$\dot{Y}_l(\vec{r}) = F_T^{-1} \left\{ \dot{U}(j\omega) \frac{\dot{S}_0^*(j\omega, \vec{r})}{\sigma^0(\vec{r}) |\dot{s}_0(j\omega)|^2 + \frac{N_{0n}}{2}} \right\}. \quad (27)$$

In (27) $\dot{U}(j\omega) = F_T \{u(t, x' = 0)\}$ and $\dot{S}_0^*(j\omega, \vec{r})$ is the spectrum of signal reflected from each point of the surface with coordinates \vec{r} . From the analysis of expression (27) it follows that the numerator corresponds to the classical method of synthesizing the aperture in the form of coordinated processing of received signals with a reference signal. The denominator describes the operation of an adaptive inverse filter with a pulse response (26). The gain of the inverse filter increases at those frequencies at which the spectral components of the received signal are reduced. As a result, the effective spectrum width of the received oscillations expands. The addition $0.5N_{0n}$ in the denominator eliminates the incorrect division by zero operation and is a regularizer of this unconventional statistical solution inverse problem of $\sigma^0(\vec{r})$ recovery. An inverse filter decorrelates the received signal making it closer to white noise.

4 EXPERIMENTS

To understand quality of proposed method of aperture synthesizing is reasonable to investigate ambiguity function. We will write (15) taking into account (3) in the following form

$$\begin{aligned}
 \dot{\Psi}(\vec{r}, \vec{r}_1) = & \int_T \dot{s}_0(t_1 - t_d(\vec{r})) \int_T \dot{s}_0^*(t_3 - t_d(\vec{r}_1)) \times \\
 & \times \int_{D'D'} \int I(x'_1) \exp(j2k\vartheta_x(\vec{r}, t_1)x'_1) \times \\
 & \times W(t_1, t_3, x'_1, x'_3, \sigma^0(\vec{r})) dx'_1 \times \\
 & \times I^*(x'_3) \exp(-j2k\vartheta_x(\vec{r}_1, t_3)x'_3) dx'_3 dt_3 dt_1 = \\
 & = \dot{s}_0(t) \otimes \left[\dot{s}_0^*(t) \otimes \left[(I(x') \exp(j2k\vartheta_x(\vec{r}, t)x')) \otimes \right. \right. \\
 & \left. \left. \otimes [W(t, x', \sigma^0(\vec{r})) \otimes I^*(x') \exp(-j2k\vartheta_x(\vec{r}, t)x')] \right] \right]. \quad (28)
 \end{aligned}$$

The two-dimensional Fourier transform in spatial and temporal coordinates of the ambiguity function takes the form

$$\begin{aligned}
 \dot{\Psi}(\omega, \vartheta_x(\vec{r}, t)) = & \\
 = & |\dot{s}_0(j\omega)|^2 |\dot{F}_{D'}(\vartheta_x(\vec{r}, t))|^2 G_W(\omega, \vartheta_x(\vec{r}, t), \sigma^0(\vec{r})). \quad (29)
 \end{aligned}$$

For the case of a discrete aperture of the onboard antenna array, the spectrum of the inverse correlation function can be factorized and written (29) in the following form

$$\begin{aligned}
 \dot{\Psi}(\omega, \vartheta_x(\vec{r}, t)) = & (|\dot{s}_0(j\omega)|^2 G_{WT}(\omega, \sigma^0(\vec{r}))) \times \\
 & \times (|\dot{F}_{D'}(\vartheta_{xl}(\vec{r}, t))|^2 G_W(\vartheta_{xl}(\vec{r}, t), \sigma^0(\vec{r}))), \quad (30)
 \end{aligned}$$

where

$$G_{WT}(\omega, \sigma^0(\vec{r})) = (\sigma^0(\vec{r}) |\dot{s}_0(j\omega)|^2 + 0.5N_{0n})^{-1}, \quad (31)$$

$$\begin{aligned}
 G_{WD'}(\vartheta_{xl}(\vec{r}, t), \sigma^0(\vec{r})) = & \\
 = & (\sigma^0(\vec{r}) |\dot{s}_0(t, \vartheta_{xl}(\vec{r}, t))|^2 + 0.5N_{0n})^{-1}. \quad (32)
 \end{aligned}$$

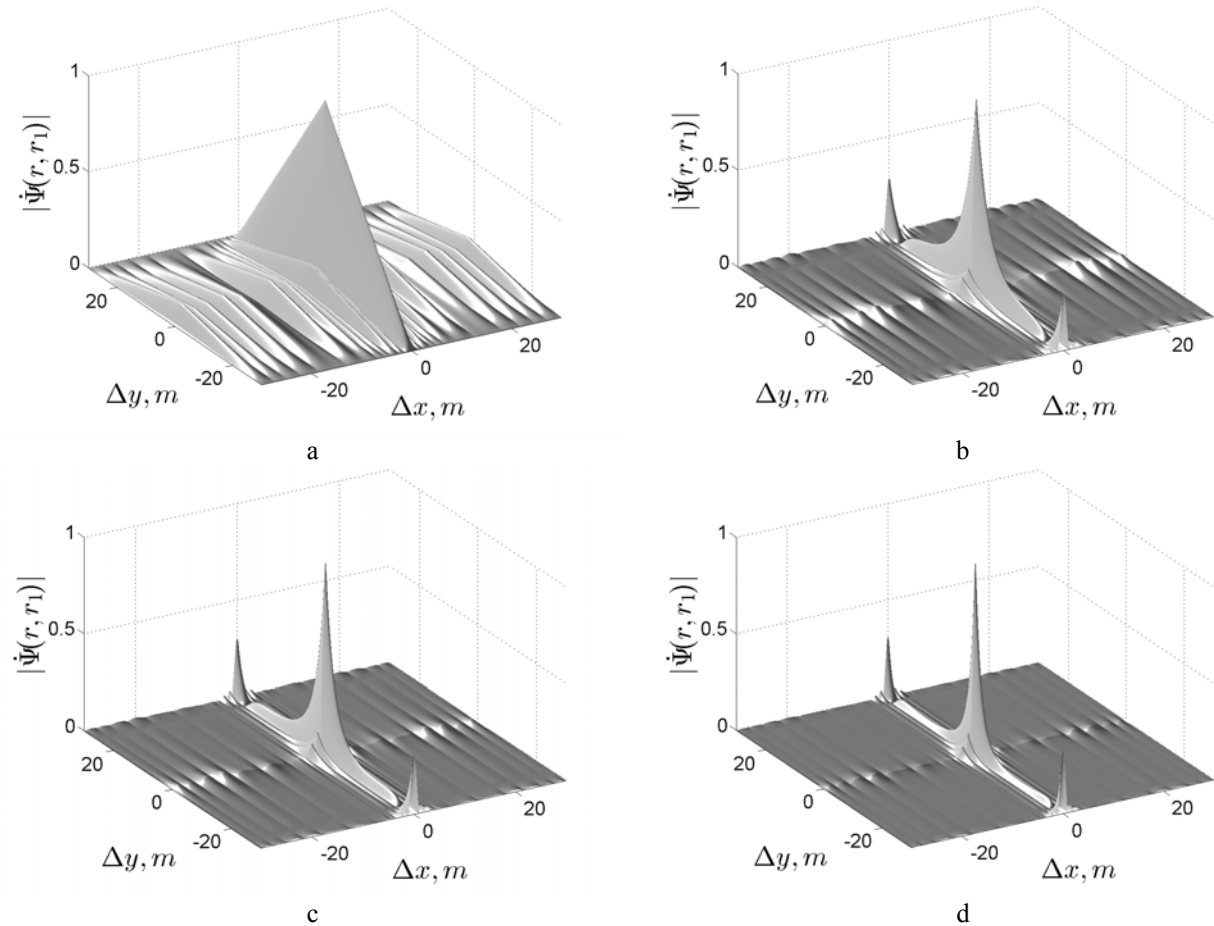


Figure 3 – Moduli of normalized ambiguity function for a sine-wave signal with a rectangular envelope and uniform amplitude-phase distribution: a – algorithm without decorrelation,
 b–d – algorithms with decorrelation and signal-to-noise ratio $2\sigma^0(\vec{r}) / N_{0n} = 10, 25, 50$

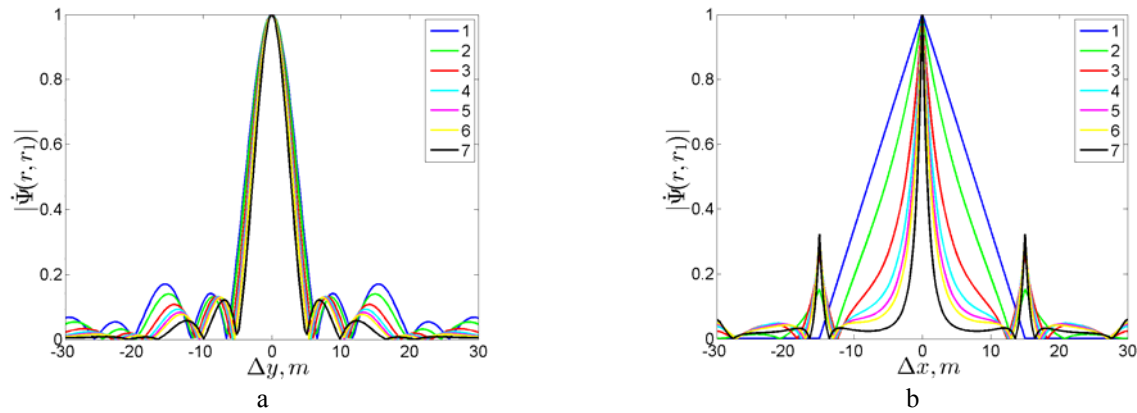


Figure 4 – The cross sections of the moduli of ambiguity functions in following coordinates: a – range, b – azimuth,
 1 – algorithm without decorrelation, (2–7) – algorithms with decorrelation and signal-to-noise ratio

$$2\sigma^0(\vec{r}) / N_{0n} = 1, 5, 10, 15, 20, 50$$

In contrast to the classical ambiguity functions the decorrelation filters make the received signals closer to white noise. In this case, the speckle dimensions are reduced in width, the number of speckles per unit area increases, which allows them to be averaged more efficiently and adaptively increase resolution with respect to the restoration of the function $\sigma^0(\vec{r})$.

Ambiguity functions $\Psi(\vec{r}, \vec{r}_1)$ and their cross sections for different signal processing algorithms are shown in Fig. 3 and Fig. 4.

For validation of proposed method it is necessary to specify observation equation correctly, i.e. model of received signal should take into account stochastic character of scattered electromagnetic field. Simulation is performed according to the scheme shown in Fig. 5.

Fig. 5 contains the following blocks: White Gaussian Noise is the block of simulation of spatial white Gaussian noise with unit variance; Test Image is test image generator, $\sqrt{0,5\sigma^0(\vec{r})}$ is the block of the test image normalization; \times is product, $+$ is sum, \otimes is two-dimensional convolution, Ambiguity Function is ambiguity function generator, $|\cdot|^2$ is square modulus, Radar Image is block of radar images visualization. In the upper and lower channel we count real $\text{Re } \dot{F}(\vec{r})$ and imaginary $\text{Im } \dot{F}(\vec{r})$ parts of the complex scattering coefficient $\dot{F}(\vec{r})$. Thereafter we form $\dot{F}(\vec{r}) = \text{Re } \dot{F}(\vec{r}) + j \text{Im } \dot{F}(\vec{r})$ and convolve it with a complex ambiguity function. At the output we form estimates of desired RCS $\sigma^0(\vec{r})$.

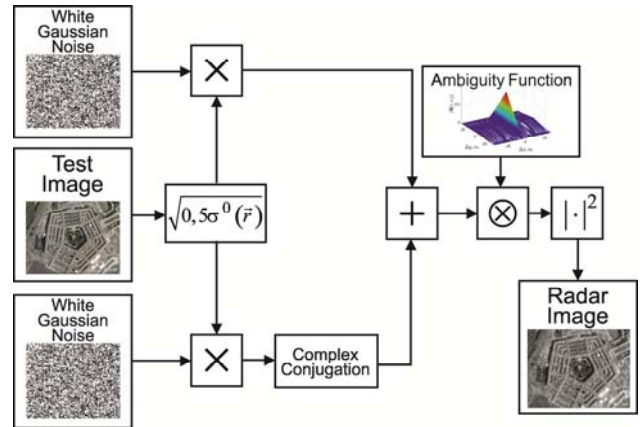


Figure 5 – The algorithm of radar images simulation

5 RESULTS

Test image is shown in Fig. 6. Fig. 7 shows a radar image formed using the classical SAR (ambiguity function in Fig. 4a) and modified algorithm (ambiguity function in Fig. 4b).



Figure 6 – Test image (RCS) $\sigma^0(\vec{r})$

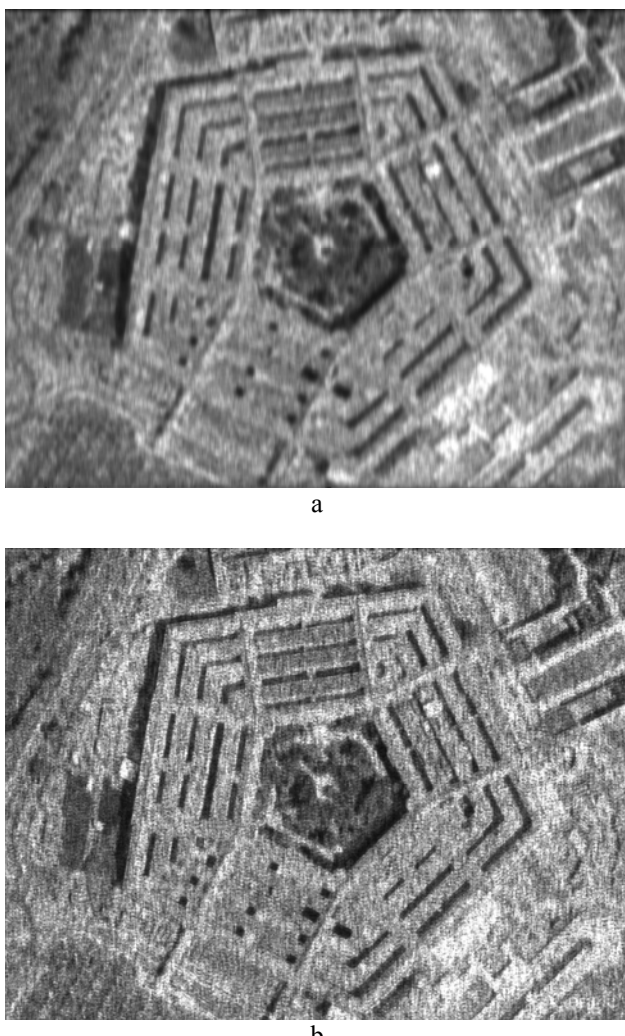


Figure 7 – Radar images reconstructed with: a – classical method, b – modified method

Images simulated using classical methods are more distorted. Resolution of modified SAR significantly exceeds the classical methods. Further image filtering by means of different rectangular windows (filters with rectangular spatial impulses response), exponential windows, Hemming weight functions, atomic functions [33, 34], median filters, Li and Frost filters allow to reduce speckle noise.

6 DISCUSSION

The obtained method (18) can be used for description of whole receiving part, means procedure of beamforming and signal processing in receiver, of cognitive radar. It is possible not only because of adaptive signals decorrelation, but also modified method of surface observation. Taking into account some restrictions it is possible to derive already well-known methods of SAR operation. We will discuss some of them.

A multi-view mode. This method is widely used in practice to compensate the speckle noise in radar images. The essence of this method is the formation of multiple rays in the azimuthal plane, the reconstruction of the RCS

surface at different angles and the summation of the shifted images. Assuming in (18) that the radiation beams are fixed in the given directions $\vartheta_{xl}(\vec{r}, t_1) = \vartheta_{xl}(\vec{r})$, we obtain the method for processing signals in a multi-view mode.

SpotLight mode. This method shows the opposite situation when one beam is formed $\vartheta_{xl}(\vec{r}, t_1) = \vartheta_{x1}(\vec{r}, t_1)$, which is focused on one fixed observation area. In this case, it is possible to achieve the highest resolution, but only local sections with the size of a spot pattern.

StripMap mode. For this mode, only one fixed beam in the direction $\vartheta_{xl}(\vec{r}, t_1) = \vartheta_{x0}(\vec{r})$ is used. This is a classic method for generating a continuous radar image with a resolution equal to the size of the aperture of a non-synthesized airborne antenna.

Scanning modes. The calculations performed in the work show that the rate of change of the angle $\vartheta_x(\vec{r}, t_1) = (x - Vt) / R_0(\vec{r}, t)$ is consistent with the velocity V of the aircraft. At the same time, with arbitrary change of the $\vartheta_x(\vec{r}, t_1)$, any of the known scanning methods can be implemented: ScanSAR, TOPS, ITOPS.

So at the stage of radar designing it is possible to choose several programs of observation based on the proposed method.

CONCLUSIONS

The problem of further developing signal processing methods of RCS estimation in SAR with linear antenna array and adaptive receiver is solved.

The scientific novelty of obtained results is that the method can satisfy two contradictory requirements to radar vision – high spatial resolution and a wide strip of the observation. The obtained optimal operations supplement already existing results with new methods and algorithms of high-precision formation of radar images, the organization of interrelations between the adaptive transmitter, the receiver, the phased array, and show potential which it is necessary to approach.

The practical significance of obtained results is that they can be used for the development of cognitive radar systems with aperture synthesizing, which country-owner will be able independently to apply, to export, lease and sell the results of observations. At the same time, the price of radar images of the required area will be defined by two factors: resolution and efficiency of imaging. These contradictory requirements to radar imaging are satisfied in this work.

Prospects for further research are to study the method of RCS estimation in SAR with planar antenna array.

ACKNOWLEDGEMENTS

The work was supported by the Ministry of Education and Science of Ukraine, the state registration number is 0120U102082.

REFERENCES

1. Gart J. Electronics and Aerospace Industry in Cold War Arizona, 1945–1968: Motorola, Hughes Aircraft, Goodyear Aircraft: thesis ... doctor of philosophy. Tempe, Arizona State University, 2006, 335 p.
2. Kreiger G., Younis M., Huber S. et al. Digital beamforming and MIMO SAR: Review and new concepts, *EUSAR : 9th European Conference, Nuremberg, 23–26 April 2012 : proceedings*. Berlin, VDE, 2012, pp. 11–14.
3. Pavlikov V. V., Nguyen K., Tymoshchuk O. M. Algorithm for radiometric imaging by ultrawideband systems of aperture synthesis, *IEEE Radar Methods and Systems Workshop, Kiev, 27–28 September 2016 : proceedings*. Kiev, IEEE, 2016, pp. 103–106. DOI:10.1109/RMSW.2016.7778561
4. Pavlikov V. V., Nguyen K., Tymoshchuk O. M. New method for the spatio-spectral sensitivity domain filling and radiometric imaging with high resolution in aperture synthesis systems, *Eurasian Journal of Mathematical and Computer Applications*, 2016, Vol. 4, Issue 4, pp. 44–53. DOI: 10.32523/2306-6172-2016-4-4-44-53
5. Pavlikov V. V., Nguyen K. Optimal algorithm for estimation of radio brightness of an extended source of radio thermal radiation in the ultra-wideband radiometric complex with a three-element-antenna system, *Modern Problems of Radio Engineering, Telecommunications and Computer Science : 13th International Conference, Lviv, 23–26 February 2016 : proceedings*. Lviv, Publishing House of Lviv Polytechnic, 2016, pp. 236–239. DOI:10.1109/TCSET.2016.7452023
6. Pavlikov V. V., Nguyen K., Tymoshchuk O. M. Optimal structural synthesis of multi-antenna ultra-wideband radiometric complex, *Physics and Engineering of Microwaves, Millimeter and Submillimeter Waves : 9th International Kharkiv Symposium, Kharkiv, 20–24 June 2016 : proceedings*. Kharkiv, IEEE, 2016, pp. 1–4. DOI:10.1109/MSMW.2016.7538181
7. Adamiuk G., Gabele M., Loinger A. et al. Technology demonstration for future DBF based spaceborne SAR missions, *EUSAR : 12th European Conference, Aachen, 4–7 June 2018 : proceedings*. Berlin, VDE, 2018, pp. 21–26.
8. Bulygin M., Baranov A., Chechina I. et al. Digital radar module for digital AESA of spaceborne SAR, *EUSAR : 12th European Conference, Aachen, 4–7 June 2018 : proceedings*. Berlin, VDE, 2018, pp. 79–82.
9. Rostan F., Rieger S., Huchler M. et al. The Sentinel-1 C-SAR Instrument Design & Performance, *EUSAR : 8th European Conference, Aachen, 7–10 June 2010 : proceedings*. Berlin, VDE, 2010, pp. 292–294.
10. Pavlikov V. V. Algorithm of optimum restoration of the radiometric image in two-antenna broadband system of aperture synthesis, *Physics and Engineering of Microwaves, Millimeter and Submillimeter Waves : 8th International Kharkov Symposium, Kharkov, 23–28 June 2013 : proceedings*. Kharkov, IEEE, 2013, pp. 605–607. DOI:10.1109/MSMW.2013.6622156
11. Pavlikov V. V. Optimal restoration of radiometric images in ultrawideband radiometric systems with multi-antenna array, *Antenna Theory and Techniques : 9th International Conference, Odessa, 16–20 September 2013 : proceedings*. Odessa, IEEE, 2013, pp. 298–300. DOI:10.1109/ICATT.2013.6650757
12. Rommel T., Rincon R., Younis M. et al. Implementation of a MIMO SAR Imaging Mode for NASA's Next Generation Airborne L-Band SAR, *EUSAR : 12th European Conference, Aachen, 4–7 June 2018 : proceedings*. Berlin, VDE, 2018, pp. 32–36.
13. Wang J., Zhu KH., Wang LN. et al. A Novel Orthogonal Waveform Separation Scheme for Airborne MIMO-SAR Systems, *Sensors*, 2018, Vol. 18, Issue 10, pp. 1–12. DOI:10.3390/s18103580
14. Marin C., Bovolo F., Bruzzone L. Building Change Detection in Multitemporal Very High Resolution SAR Images, *IEEE Transactions on Geoscience and Remote Sensing*, 2015, Vol. 53, Issue 5, pp. 2664–2682. DOI: 10.1109/TGRS.2014.2363548
15. Cho J. H., Park C. G. Multiple Feature Aggregation Using Convolutional Neural Networks for SAR Image-Based Automatic Target Recognition, *IEEE Geoscience and Remote Sensing Letters*, 2018, Vol. 15, Issue 12, pp. 1882–1886.
16. Buck C., Gebert N., Angevain J. C. et al. An Overview of ESA Activities in Support of Direct Ocean Surface Current Measurement from Space, *EUSAR : 12th European Conference, Aachen, 4–7 June 2018 : proceedings*. Berlin, VDE, 2018, pp. 1417–1422.
17. Damini A., McDonald M., Haslam G. E. X-band wideband experimental airborne radar for SAR, GMTI and maritime surveillance, *IEE Proceedings – Radar, Sonar and Navigation*, 2003, Vol. 150, Issue 4, pp. 305–312. DOI: 10.1049/ip-rsn:20030654
18. Xinze Y., Jianqiang L., Chunhua X., Tao Z. et al. Application of spaceborne SAR imagery in monitoring green algae, *APSAR : 2nd Asian-Pacific Conference, Xian, 26–30 October 2009 : proceedings*. Xian, IEEE, 2009, pp. 129–131. DOI: 10.1109/APSAR.2009.5374140
19. Brunner D., Schulz K., Brehm T. Building damage assessment in decimeter resolution SAR imagery: A future perspective, *Joint Urban Remote Sensing Event, Munich, 11–13 April 2011*. Munich, IEEE, 2011, pp. 217–220. DOI: 10.1109/JURSE.2011.5764759
20. Maksymiuk O., Schmitt M., Brenner A. R. et al. First investigations on detection of stationary vehicles in airborne decimeter resolution SAR data by supervised learning, *IEEE International Geoscience and Remote Sensing Symposium, Munich, 22–27 July 2012 : proceedings*. Munich, IEEE, 2012, pp. 3584–3587. DOI: 10.1109/IGARSS.2012.6350642
21. Stilla U., Schmitt M., Maksymiuk O. et al. Towards the recognition of individual trees in decimeter-resolution airborne millimeterwave SAR, *Pattern Recognition in Remote Sensing : 8th IAPR Workshop, Stockholm, 24 August 2014 : proceedings*. Stockholm, IEEE, 2014, pp. 48–51. DOI: 10.1109/PRRS.2014.6914287
22. Baqué R., Castet N., Fromage P. et al. Ultra-High Resolution and Long Range X-Band Airborne SAR System, *International Conference on Radar, Brisbane, 27–31 August 2018 : proceedings*. Brisbane, IEEE, 2018, pp. 388–393. DOI: 10.1109/RADAR.2018.8557220
23. Baqué R., Castet N., Fromage P. et al. SETHI/RAMSES-NG new performances of the flexible multi-spectral airborne remote sensing research platform, *International Conference on Radar Systems, Nuremberg, 11–13 October 2017 : proceedings*. Nuremberg, IEEE, 2017, pp. 191–194.
24. Krieger G., Huber S., Villano M. et al. SIMO and MIMO System Architectures and Modes for High-Resolution Ultra-Wide-Swath SAR Imaging, *EUSAR : 11th European Conference on Synthetic Aperture Radar, Hamburg, 6–9 June 2016 : proceedings*. Berlin, VDE, 2016, pp. 1–6.
25. Krieger G., Huber S., Younis M. et al. In-Orbit Relative Amplitude and Phase Antenna Pattern Calibration for

- Tandem-L, *EUSAR : 12th European Conference on Synthetic Aperture Radar, Aachen, 4–7 June 2018 : proceedings*. Berlin, VDE, 2018, pp. 421–426.
26. Volosyuk V. K., Pavlikov V. V., Zhyla S. S. Phenomenological Description of the Electromagnetic Field and Coherent Images in Radio Engineering and Optical Systems, *Mathematical Methods in Electromagnetic Theory : 17th International Conference, Kiev, 2–5 July 2018: proceedings*. Kiev, IEEE, 2018, pp. 302–305. DOI: 10.1109/MMET.2018.8460321
27. Volosyuk V. K., Zhila S. S., Kolesnikov D. V. Phenomenological description of coherent radar images based on the concepts of the measure of set and stochastic integral, *Telecommunications and Radio Engineering*, 2019, Vol. 78, Issue 1, pp. 19–30. DOI: 10.1615/TelecomRadEng.v78.i1.30
28. Volosyuk V. K., Kravchenko V. F. Statistical Theory of Radio-Engineering Systems of Remote Sensing and Radar. Moscow, Fizmatlit, 2008, 704 p.
29. Kravchenko V. F., Kutuza B. G., Volosyuk V. K. et al. Super-resolution SAR imaging: Optimal algorithm synthesis and simulation results, *Progress in Electromagnetics Research Symposium, St. Petersburg, 22–25 May 2017 : proceedings*. St. Petersburg, IEEE, 2017, pp. 419–452. DOI: 10.1109/PIERS.2017.8261776
30. Volosyuk V. K., Zhyla S. S. Optimal radar cross section estimation in synthetic aperture radar, *Electrical and Computer Engineering : 1st Ukraine Conference, Kiev, 29 May – 2 June 2017 : proceedings*. Kiev, IEEE, 2017, pp. 189–193. DOI: 10.1109/UKRCON.2017.8100471
31. Volosyuk V. K., Zhyla S. S., Antonov M. O. et al. Optimal acquisition mode and signal processing algorithm in synthetic aperture radar, *Electronics and Nanotechnology : 37th International Conference, Kiev, 18–20 April 2017 : proceedings*. Kiev, IEEE, 2017, pp. 511–516. DOI: 10.1109/ELNANO.2017.7939804
32. Pavlikov V. V., Volosyuk V. K., Zhyla S. S. et al. Active Aperture Synthesis Radar for High Spatial Resolution Imaging, *Ultrawideband and Ultrashort Impulse Signals : 9th International Conference, Odessa, 4–7 September 2018 : proceedings*. Odessa, IEEE, 2018, pp. 252–255. DOI: 10.1109/UWBUSIS.2018.8520021
33. Blednov V. I., Pavlikov V. V., Jakuschenko I. Filtration of the radar images by filters with weighting coefficients of classical and new Kravchenko windows, *Physics and Engineering of Microwaves, Millimeter and Submillimeter Waves and Workshop on Terahertz Technologies : 6th International Kharkov Symposium, Kharkov, 25–30 June 2007 : proceedings*. Kharkov, IEEE, 2007, pp. 986–988. DOI: 10.1109/MSMW.2007.4294883
34. Pavlikov V. V. Application of Kravchenko windows in problems of formation of the radar subsurface layers images by the onboard radar of subsurface sensing, *Physics and Engineering of Microwaves, Millimeter and Submillimeter Waves and Workshop on Terahertz Technologies : 6th International Kharkov Symposium, Kharkov, 25–30 June 2007 : proceedings*. Kharkov, IEEE, 2007, pp. 938–940. DOI: 10.1109/MSMW.2007.4294867

Received 14.05.2020.
Accepted 10.09.2020.

УДК 621.396

ПОБУДОВА ЗОБРАЖЕННЯ ЕФЕКТИВНОЇ ПЛОЩІ РОЗСІЯННЯ В РАДАРІ З СИНТЕЗОВАНОЮ АПЕРТУРОЮ АНТЕНІ, ЛІНІЙНОЮ АНТЕННОЮ РЕШІТКОЮ І АДАПТИВНИМ ПРИЙМАЧЕМ

Волосюк В. К. – д-р техн. наук, професор кафедри аерокосмічних радіоелектронних систем Національного аерокосмічного університету «Харківський авіаційний інститут», Харків, Україна.

Жила С. С. – канд. техн. наук, завідувач кафедри аерокосмічних радіоелектронних систем Національного аерокосмічного університету «Харківський авіаційний інститут», Харків, Україна.

Руженцев М. В. – д-р техн. наук, професор, Провідний науковий співробітник кафедри аерокосмічних радіоелектронних систем Національного аерокосмічного університету «Харківський авіаційний інститут», Харків, Україна.

Собколов А. Д. – аспірант кафедри аерокосмічних радіоелектронних систем, Національного аерокосмічного університету «Харківський авіаційний інститут» Харків, Україна.

Церне Е. О. – асистент кафедри аерокосмічних радіоелектронних систем Національного аерокосмічного університету «Харківський авіаційний інститут», Харків, Україна.

Колесников Д. В. – інженер кафедри аерокосмічних радіоелектронних систем Національного аерокосмічного університету «Харківський авіаційний інститут», Харків, Україна.

Власенко Д. С. – асистент кафедри аерокосмічних радіоелектронних систем Національного аерокосмічного університету «Харківський авіаційний інститут», Харків, Україна.

Топал М. С. – доцент кафедри проектування літаків та вертолітів Національного аерокосмічного університету «Харківський авіаційний інститут», Харків, Україна.

АНОТАЦІЯ

Актуальність. Існує велика кількість методів оцінки ЕПР в бортових радах з синтезом апертури, які відрізняються точністю, часом відновлення ЕПР заданої області і складністю реалізації. У той же час оптимальний метод, який є узагальненням всіх існуючих і який характеризує як просторову, так і часову оптимальну обробку сигналів синтезований не був. Тож при постановці більшості завдань не враховується стохастична структура сигналів, відбитих від більшості підстилаючих поверхонь. В результаті не визначені подальші шляхи покращення роздільної здатності, оптимальна структура радара з синтезуванням апертури антени і гранично досяжна точність оцінювання ЕПР.

Мета. Метою роботи є рішення наскрізної задачі синтезу оптимального методу відновлення ЕПР поверхонь, як статистичної характеристики просторово-неоднорідних випадкових процесів, в радіотехнічних системах аерокосмічного базування з рухомими лінійними антенними решітками і адаптивною просторово-часовою обробкою сигналів.

Метод. Використовуючи метод максимальної правдоподібності та враховуючи апріорну інформацію про статистичні характеристики прийнятих просторово-часових полів, отриманий метод надзвірізначення оцінки ЕПР за просторовими коор-

динатам. Узагальнена постановка задачі дозволила визначити оптимальний метод спостереження поверхні, що дозволяє подолати протиріччя між розміром зони спостереження і точністю оцінок параметрів. Отриманий метод дозволяє досягнути найкращого розрізнення (як в прожекторному режимі) радіолокаційних зображень для широкої області спостереження (такої, як в смуговому режимі). Показано, що загальний алгоритм можна адаптувати до часткових розв'язків з обмеженими постановками завдання. На відміну від відомого методу синтезу апертури обробка прийнятого поля в антенній решітці і приймачі є адаптивною і залежить від відношення сигнал/шум.

Результати. Оптимальний метод сканування області спостереження на борту РСА з антенними решітками і відповідний метод адаптивної просторово-часової обробки сигналу можуть бути використані для опису роботи вхідного тракту приймачів когнітивного бортового радара дистанційного зондування.

Висновки. Отриманий оптимальний метод можна розглядати як модифікований метод синтезування апертури з багатопроменевим прожекторним оглядом і можливістю адаптивного діаграмоутворення, і часовою обробкою сигналів. На відміну від класичного методу, який здійснює узгоджену фільтрацію прийнятого сигналу з опорним сигналом, в модифікованому методі додатково здійснюється декореляції сигналів, відбитих від земної поверхні. В результаті такої декореляції характерні інтервали спеклів (розміри плямистої структури зображення) будуть значно менше, ніж при узгодженні фільтрації. Тому їх подальше згладжування з тією ж ефективністю може бути виконано вікнами меншої ширини. Це в підсумку в результаті спільно з багатопроменевим прожекторним оглядом дозволить значно підвищити роздільну здатність РСА з розширеною областю спостереження.

Ключові слова: радар з синтезованою апертурою, ефективна площа розсіювання, статистична оптимізація, оптимальний режим огляду поверхні, надроздільний метод, когнітивні радари.

УДК 621.396

ПОСТРОЕНИЕ ИЗОБРАЖЕНИЯ ЭФФЕКТИВНОЙ ПЛОЩАДИ РАССЕЯНИЯ В РАДАРЕ С СИНТЕЗИРОВАННОЙ АПЕРТУРОЙ АНТЕННЫ, ЛИНЕЙНОЙ АНТЕННОЙ РЕШЕТКОЙ И АДАПТИВНЫМ ПРИЕМНИКОМ

Волосюк В. К. – д-р техн. наук, профессор кафедры аэрокосмических радиоэлектронных систем Национального аэрокосмического университета «Харьковский авиационный институт», Харьков, Украина.

Жила С. С. – канд. техн. наук, заведующий кафедры аэрокосмических радиоэлектронных систем Национального аэрокосмического университета «Харьковский авиационный институт», Харьков, Украина.

Руженцев Н. В. – д-р техн. наук, профессор, ведущий научный сотрудник кафедры аэрокосмических радиоэлектронных систем Национального аэрокосмического университета «Харьковский авиационный институт», Харьков, Украина.

Собковов А. Д. – аспирант кафедры аэрокосмических радиоэлектронных систем Национального аэрокосмического университета «Харьковский авиационный институт», Харьков, Украина.

Цернэ Э. А. – ассистент кафедры аэрокосмических радиоэлектронных систем Национального аэрокосмического университета «Харьковский авиационный институт», Харьков, Украина.

Колесников Д. В. – инженер кафедры аэрокосмических радиоэлектронных систем Национального аэрокосмического университета «Харьковский авиационный институт», Харьков, Украина.

Власенко Д. С. – ассистент кафедры аэрокосмических радиоэлектронных систем Национального аэрокосмического университета «Харьковский авиационный институт», Харьков, Украина.

Топал Н. С. – доцент кафедры проектирования самолетов и вертолетов Национального аэрокосмического университета «Харьковский авиационный институт», Харьков, Украина.

АННОТАЦИЯ

Актуальность. Существует значительное количество методов оценки ЭПР в бортовых радах с синтезом апертуры, которые отличаются точностью, временем восстановления ЭПР заданной области и сложностью реализации. В тоже время оптимальный метод, являющийся обобщением всех существующих и характеризующий как пространственную, так и временную оптимальную обработку сигналов синтезирован не был. Также при постановке большинства задач не учитывается стохастическая структура сигналов, отраженных от большинства подстилающих поверхностей. В результате не определены дальнейшие пути улучшения разрешающей способности, оптимальная структура радара с синтезированием апертуры антенны и предельно достижимая точность оценивания ЭПР.

Цель. Целью работы является решение сквозной задачи синтеза оптимального метода восстановления ЭПР поверхностей, как статистической характеристики пространственно-неоднородных случайных процессов, в радиотехнических системах аэрокосмического базирования с движущимися линейными антенными решетками и адаптивной пространственно-временной обработкой сигналов.

Метод. Используя метод максимального правдоподобия и учитывая априорную информацию о статистических характеристиках принятых пространственно-временных полей, получен метод сверхразрешения оценки ЭПР по пространственным координатам. Обобщенная постановка задачи позволила определить оптимальный метод наблюдения поверхности, позволяющий преодолеть противоречие между размером зоны наблюдения и точностью оценок параметров. Полученный метод позволяет добиться наилучшего разрешения (как в прожекторном режиме) радиолокационных изображений для широкой области наблюдения (такой, как в полосовом режиме). Показано, что общий алгоритм можно адаптировать к частным решениям с ограниченными постановками задачи. В отличие от известного метода синтеза апертуры обработка принимаемого поля в антенной решетке и приемнике является адаптивной и зависит от отношения сигнал/шум.

Результаты. Оптимальный метод сканирования области наблюдения на борту РСА с антенными решетками и соответствующий метод адаптивной пространственно-временной обработки сигнала могут быть использованы для описания работы входного тракта приемников когнитивного бортового радара дистанционного зондирования.

Выводы. Полученный оптимальный метод можно рассматривать как модифицированный метод синтезирования апертуры с многолучевым прожекторным обзором и возможностью адаптивного диаграммообразования и временной обработкой сигналов. В отличие от классического метода, осуществляющего согласованную фильтрацию принятого сигнала с опорным сигналом, в модифицированном методе дополнительно осуществляется декорреляция сигналов, отраженных от земной поверхности. В результате такой декорреляции характерные интервалы спеклов (размеры пятнистой структуры изображения) будут значительно меньше, чем при согласованной фильтрации. Поэтому их последующее сглаживание с той же эффективностью может быть выполнено окнами меньшей ширины. Это, в конечном итоге, совместно с многолучевым прожекторным обзором позволит значительно повысить разрешающую способность РСА с расширенной областью наблюдения.

Ключевые слова: радар с синтезированной апертурой, эффективная площадь рассеяния, статистическая оптимизация, оптимальный режим обзора поверхности, сверхразрешающий метод, когнитивные радары.

ЛІТЕРАТУРА / ЛІТЕРАТУРА

1. Gart J. Electronics and Aerospace Industry in Cold War Arizona, 1945–1968: Motorola, Hughes Aircraft, Goodyear Aircraft: thesis ... doctor of philosophy / Gart Jason. – Tempe: Arizona State University, 2006. – 335 p.
2. Digital beamforming and MIMO SAR: Review and new concepts / [G. Kreiger, M. Younis, S. Huber et al.] // EUSAR : 9th European Conference, Nuremberg, 23–26 April 2012 : proceedings. – Berlin : VDE, 2012. – P. 11–14.
3. Pavlikov V. V. Algorithm for radiometric imaging by ultrawideband systems of aperture synthesis / V. V. Pavlikov, K. Nguyen, O. M. Tymoshchuk // IEEE Radar Methods and Systems Workshop, Kiev, 27–28 September 2016 : proceedings. – Kiev : IEEE, 2016. – P. 103–106. DOI:10.1109/RMSW.2016.7778561
4. Pavlikov V. V. New method for the spatio-spectral sensitivity domain filling and radiometric imaging with high resolution in aperture synthesis systems / V. V. Pavlikov, K. Nguyen, O. M. Tymoshchuk // Eurasian Journal of Mathematical and Computer Applications. – 2016. – Vol. 4, Issue 4. – P. 44–53. DOI:10.32523/2306-6172-2016-4-4-44-53
5. Pavlikov V. V. Optimal algorithm for estimation of radio brightness of an extended source of radio thermal radiation in the ultra-wideband radiometric complex with a three-element-antenna system / V. V. Pavlikov, K. Nguyen // Modern Problems of Radio Engineering, Telecommunications and Computer Science : 13th International Conference, Lviv, 23–26 February 2016 : proceedings. – Lviv : Publishing House of Lviv Polytechnic, 2016. – P. 236–239. DOI:10.1109/TCSET.2016.7452023
6. Pavlikov V. V. Optimal structural synthesis of multi-antenna ultra-wideband radiometric complex / V. V. Pavlikov, K. Nguyen, O. M. Tymoshchuk // Physics and Engineering of Microwaves, Millimeter and Submillimeter Waves : 9th International Kharkiv Symposium, Kharkiv, 20–24 June 2016 : proceedings. – Kharkiv : IEEE, 2016. – P. 1–4. DOI:10.1109/MSMW.2016.7538181
7. Technology demonstration for future DBF based spaceborne SAR missions / [G. Adamiuk, M. Gabele, A. Loinger et al.] // EUSAR : 12th European Conference, Aachen, 4–7 June 2018 : proceedings. – Berlin : VDE, 2018. – P. 21–26.
8. Digital radar module for digital AESA of spaceborne SAR / [M. Bulygin, A. Baranov, I. Chechina et al.] // EUSAR : 12th European Conference, Aachen, 4–7 June 2018 : proceedings. – Berlin: VDE, 2018. – P. 79–82.
9. The Sentinel-1 C-SAR Instrument Design & Performance / [F. Rostan, S. Riegger, M. Huchler et al.] // EUSAR : 8th European Conference, Aachen, 7–10 June 2010 : proceedings. – Berlin : VDE, 2010. – P. 292–294.
10. Pavlikov V. V. Algorithm of optimum restoration of the radiometric image in two-antenna broadband system of aperture synthesis / V. V. Pavlikov // Physics and Engineering of Microwaves, Millimeter and Submillimeter Waves : 8th International Kharkov Symposium, Kharkov, 23–28 June 2013 : proceedings. – Kharkov : IEEE, 2013. – P. 605–607. DOI:10.1109/MSMW.2013.6622156
11. Pavlikov V. V. Optimal restoration of radiometric images in ultrawideband radiometric systems with multi-antenna array / V. V. Pavlikov // Antenna Theory and Techniques : 9th International Conference, Odessa, 16–20 September 2013 : proceedings. – Odessa : IEEE, 2013. – P. 298–300. DOI:10.1109/ICATT.2013.6650757
12. Implementation of a MIMO SAR Imaging Mode for NASA's Next Generation Airborne L-Band SAR / [T. Rommel, R. Rincon, M. Younis et al.] // EUSAR : 12th European Conference, Aachen, 4–7 June 2018 : proceedings. – Berlin : VDE, 2018. – P. 32–36.
13. A Novel Orthogonal Waveform Separation Scheme for Airborne MIMO-SAR Systems / [J Wang, KH Zhu, LN Wang et al.] // Sensors. – 2018. – Vol. 18, Issue 10. – P. 1–12. DOI:10.3390/s18103580
14. Marin C. Building Change Detection in Multitemporal Very High Resolution SAR Images / C. Marin, F. Bovolo, L. Bruzzone // IEEE Transactions on Geoscience and Remote Sensing. – 2015. – Vol. 53, Issue 5. – P. 2664–2682. DOI:10.1109/TGRS.2014.2363548
15. Cho J. H. Multiple Feature Aggregation Using Convolutional Neural Networks for SAR Image-Based Automatic Target Recognition / J. H. Cho, C. G. Park // IEEE Geoscience and Remote Sensing Letters. – 2018. – Vol. 15, Issue 12. – P. 1882–1886.
16. An Overview of ESA Activities in Support of Direct Ocean Surface Current Measurement from Space / [C. Buck, N. Gebert, J. C. Angevine et al.] // EUSAR : 12th European Conference, Aachen, 4–7 June 2018 : proceedings. – Berlin : VDE, 2018. – P. 1417–1422.
17. Damini A. X-band wideband experimental airborne radar for SAR, GMTI and maritime surveillance / A. Damini, M. McDonald, G. E. Haslam // IEE Proceedings – Radar, Sonar and Navigation. – 2003. – Vol. 150, Issue 4. – P. 305–312. DOI:10.1049/ip-rsn:20030654
18. Application of spaceborne SAR imagery in monitoring green algae / [Y. Xinzhe, L. Jianqiang, X. Chunhua, Z. Tao et al.] // APSAR : 2nd Asian-Pacific Conference, Xian, 26–30 October 2009 : proceedings. – Xian : IEEE, 2009. – P. 129–131. DOI: 10.1109/APSAR.2009.5374140
19. Brunner D. Building damage assessment in decimeter resolution SAR imagery: A future perspective / D. Brunner, K. Schulz, T. Brehm // Joint Urban Remote Sensing Event,

- Munich, 11–13 April 2011. – Munich : IEEE, 2011. – P. 217–220. DOI: 10.1109/JURSE.2011.5764759
20. First investigations on detection of stationary vehicles in airborne decimeter resolution SAR data by supervised learning / [O. Maksymiuk, M. Schmitt, A. R. Brenner et al.] // IEEE International Geoscience and Remote Sensing Symposium, Munich, 22–27 July 2012 : proceedings. – Munich: IEEE, 2012. – P. 3584–3587. DOI: 10.1109/IGARSS.2012.6350642
21. Towards the recognition of individual trees in decimeter-resolution airborne millimeterwave SAR / [U. Stilla, M. Schmitt, O. Maksymiuk et al.] // Pattern Recognition in Remote Sensing : 8th IAPR Workshop, Stockholm, 24 August 2014 : proceedings. – Stockholm: IEEE, 2014. – P. 48–51. DOI: 10.1109/PRRS.2014.6914287
22. Ultra-High Resolution and Long Range X-Band Airborne SAR System / [R. Baqué, N. Castet, P. Fromage et al.] // International Conference on Radar, Brisbane, 27–31 August 2018 : proceedings. – Brisbane : IEEE, 2018. – P. 388–393. DOI: 10.1109/RADAR.2018.8557220
23. SETHI/RAMSES-NG new performances of the flexible multi-spectral airborne remote sensing research platform / [R. Baqué, N. Castet, P. Fromage et al.] // International Conference on Radar Systems, Nuremberg, 11–13 October 2017: proceedings. – Nuremberg: IEEE, 2017. – P. 191–194.
24. SIMO and MIMO System Architectures and Modes for High-Resolution Ultra-Wide-Swath SAR Imaging / [G. Krieger, S. Huber, M. Villano et al.] // EUSAR : 11th European Conference on Synthetic Aperture Radar, Hamburg, 6–9 June 2016 : proceedings. – Berlin : VDE, 2016. – P. 1–6.
25. In-Orbit Relative Amplitude and Phase Antenna Pattern Calibration for Tandem-L / [G. Krieger, S. Huber, M. Younis et al.] // EUSAR : 12th European Conference on Synthetic Aperture Radar, Aachen, 4–7 June 2018 : proceedings. – Berlin: VDE, 2018. – P. 421–426.
26. Volosyuk V. K. Phenomenological Description of the Electromagnetic Field and Coherent Images in Radio Engineering and Optical Systems / V. K. Volosyuk, V. V. Pavlikov, S. S. Zhyla // Mathematical Methods in Electromagnetic Theory : 17th International Conference, Kiev, 2–5 July 2018: proceedings. – Kiev : IEEE, 2018. – P. 302–305. DOI: 10.1109/MMET.2018.8460321
27. Volosyuk V. K. Phenomenological description of coherent radar images based on the concepts of the measure of set and stochastic integral / V. K. Volosyuk, S. S. Zhila, D. V. Kolesnikov // Telecommunications and Radio Engineering. – 2019. – Vol. 78, Issue 1. – P. 19–30. DOI: 10.1615/TelecomRadEng.v78.i1.30
28. Volosyuk V. K. Statistical Theory of Radio-Engineering Systems of Remote Sensing and Radar / V. K. Volosyuk, V. F. Kravchenko. – Moscow : Fizmatlit, 2008. – 704 p.
29. Super-resolution SAR imaging: Optimal algorithm synthesis and simulation results / [V. F. Kravchenko, B. G. Kutuza, V. K. Volosyuk et al.] // Progress in Electromagnetics Research Symposium, St. Petersburg, 22–25 May 2017 : proceedings. – St. Petersburg : IEEE, 2017. – P. 419–452. DOI: 10.1109/PIERS.2017.8261776
30. Volosyuk V. K. Optimal radar cross section estimation in synthetic aperture radar / V. K. Volosyuk, S. S. Zhyla // Electrical and Computer Engineering : 1st Ukraine Conference, Kiev, 29 May – 2 June 2017 : proceedings. – Kiev : IEEE, 2017. – P. 189–193. DOI: 10.1109/UKRCON.2017.8100471
31. Optimal acquisition mode and signal processing algorithm in synthetic aperture radar / [V. K. Volosyuk, S. S. Zhyla, M. O. Antonov et al.] // Electronics and Nanotechnology : 37th International Conference, Kiev, 18–20 April 2017 : proceedings. – Kiev : IEEE, 2017. – P. 511–516. DOI: 10.1109/ELNANO.2017.7939804
32. Active Aperture Synthesis Radar for High Spatial Resolution Imaging / [V. V. Pavlikov, V. K. Volosyuk, S. S. Zhyla et al.] // Ultrawideband and Ultrashort Impulse Signals : 9th International Conference, Odessa, 4–7 September 2018 : proceedings. – Odessa : IEEE, 2018. – P. 252–255. DOI: 10.1109/UWBUSIS.2018.8520021
33. Blednov V. I. Filtration of the radar images by filters with weighting coefficients of classical and new Kravchenko windows / V. I. Blednov, V. V. Pavlikov, I. Jakuschenko // Physics and Engineering of Microwaves, Millimeter and Submillimeter Waves and Workshop on Terahertz Technologies : 6th International Kharkov Symposium, Kharkov, 25–30 June 2007 : proceedings. – Kharkov : IEEE, 2007. – P. 986–988. DOI: 10.1109/MSMW.2007.4294883
34. Pavlikov V. V. Application of Kravchenko windows in problems of formation of the radar subsurface layers images by the onboard radar of subsurface sensing / V. V. Pavlikov // Physics and Engineering of Microwaves, Millimeter and Submillimeter Waves and Workshop on Terahertz Technologies : 6th International Kharkov Symposium, Kharkov, 25–30 June 2007 : proceedings. – Kharkov : IEEE, 2007. – P. 938–940. DOI: 10.1109/MSMW.2007.4294867